scientific reports

Check for updates

OPEN

Analysis of dynamic network reconfiguration in HIV patients with cognitive impairment based multilayer network

Xingyuan Jiang[1,4], Juming Ma[1,4], Chuanke Hou[1,4] & Hongjun Li[1,2,3]✉

Approximately half of HIV patients continue to experience HIV-associated neurocognitive disorders (HAND). Our study aims to evaluate changes in the dynamic activity patterns of functional brain communities in the early stages of HIV infection by comparing time-varying multilayer network metrics. A total of 165 persons living with HIV but without neurocognitive disorders (PWND), 173 individuals with asymptomatic neurocognitive impairment (ANI), and 100 matched healthy controls (HC) were enrolled. A time-varying multilayer network model was constructed, and global modularity (Q value) and nodal flexibility were calculated using different parameter settings (γ = [0.9, 1, 1.1], ω = [0.5, 0.75, 1]). Brain functional alterations in the PWND and ANI groups were evaluated from both global and nodal perspectives. Associations between network measures, clinical variables, and cognitive performance were also explored. Using the full connectivity matrix, no significant differences in global modularity (Q value) were found among the three groups. However, when thresholding the matrix to retain the top 10% of strongest connections, the ANI group showed significantly lower modularity than the HC group across all γ and ω combinations ($p < 0.05$). At γ = 0.9 and ω = 0.5, reduced nodal flexibility was observed in visual network regions in the PWND group, while the ANI group showed reduced flexibility in regions belonging to the default mode network (DMN), sensorimotor network (SMN), and limbic network (LIM). At γ = 0.9 and ω = 1, the ANI group exhibited increased flexibility in DMN regions compared to HC. Additionally, thresholding the top 10% connections revealed increased flexibility in the right lingual gyrus (visual network) in ANI compared to HC (FDR corrected, $p < 0.05$). Nodal flexibility was positively correlated with neurocognitive performance in the PWND group, whereas a significant negative correlation was observed in the ANI group. Regardless of cognitive impairment, HIV patients exhibit abnormalities in dynamic community structures. These findings provide new insights and perspectives for the early detection of brain damage, advancing our current understanding of time-varying multilayer networks in HIV patients.

Keywords HIV-associated neurocognitive disorders, Resting-state fMRI, Time-varying multilayer network, Global modularity, Node flexibility

With the widespread use of combination antiretroviral treatment (cART), AIDS has transformed into a chronic disease. However, approximately half of people living with HIV (PLWH) gradually experience cognitive and motor function decline, leading to the development of HIV-associated neurocognitive disorders (HAND)[1,2]. Asymptomatic neurocognitive impairment (ANI) represents the early stage and the most common form of HAND, marking a crucial, reversible period for the prevention and intervention of HAND[3,4]. Regular screening using HAND scales is an effective tool for the early diagnosis and monitoring of neurocognitive function, as well as for evaluating treatment efficacy. However, in clinical practice, these scales face several challenges, including being time-consuming, having low thresholds, and being highly subjective. Moreover, they are not suitable for assessing the extent of brain injury in persons living with HIV but without neurocognitive disorders (PWND). Functional magnetic resonance imaging (fMRI) technology potentially offers a non-invasive and precise method

[1]Department of Radiology, Beijing YouAn Hospital, Capital Medical University, Beijing, China. [2]Beijing Advanced Innovation Centre for Biomedical Engineering, Beihang University, Beijing, China. [3]Laboratory for Clinical Medicine, Capital Medical University, Beijing, China. [4]Xingyuan Jiang, Juming Ma and Chuanke Hou: These authors contributed equally to this work as co-first authors. ✉email: lihongjun00113@ccmu.edu.cn

to detect early brain injury in PLWH, investigate the patterns and mechanisms of HAND development and progression, and identify promising alternative biomarkers.

Previous studies have reported abnormalities in the static, single-layer topological structure of brain functional networks following HIV infection[5–7], suggesting that HAND is a network disorder. Recently, the multilayer network model has garnered significant attention in neuroscience due to its ability to capture comprehensive information from multimodal, multiscale, multifrequency, and spatiotemporal datasets[8,9]. Additionally, research has demonstrated that the brain undergoes numerous changes over short time scales[10,11], making dynamic network analysis a burgeoning area of study. Several studies have revealed that dynamic functional networks can uncover complex and dynamic interaction patterns between different brain regions that static networks overlook[10,12,13].

Time-varying multilayer networks, which describe temporal flows between adjacent network layers[11], represent a typical model of multilayer networks with both node and temporal dimensions. Mangor et al.[14] applied the time-varying multilayer network model to resting-state fMRI data from healthy subjects, finding that it effectively predicts healthy individuals' behavior and brain performance.

To facilitate the study of community structures in multilayer network models, Mucha et al.[15] first introduced a multilayer community detection quality function based on single-layer network community detection. This function evaluates the quality of communities within multilayer networks and introduced modularity as a global metric. In 2011, Danielle et al.[16] proposed using flexibility to measure the frequency of nodes changing their associated communities. They found that during learning processes, the frequency with which nodes switch communities can predict subsequent learning outcomes in the brain. Currently, methods for studying community structure changes using multilayer networks are gradually being applied to research on neurological disorders, yielding some exciting results. The earliest application was in 2016, when a study on schizophrenia found that patients exhibited higher network flexibility compared to healthy controls, indicating greater disorganization during community restructuring in patients' brains[17]. In 2018, He et al.[18] discovered disrupted dynamic network reconfiguration in the language system of patients with temporal lobe epilepsy. They suggested that, compared to traditional task-based static measures, dynamic network reconfiguration analysis based on multilayer networks provides higher predictive accuracy for epilepsy. These findings suggest that studying dynamic brain network reconfigurations using time-varying multilayer networks can yield novel insights, potentially aiding in understanding the pathogenesis of psychiatric disorders and identifying potential biomarkers for auxiliary diagnosis.

To reduce confounding effects related to aging, this study specifically selected young Chinese men who have sex with men (MSM) as participants, as HAND-related brain changes may be more pronounced and detectable in a relatively homogeneous younger cohort. Participants were divided into three groups: ANI, PWND, and normal controls (NCs). For the first time, the study applied time-varying multilayer networks to patients with HIV-associated cognitive impairment, calculating global metrics (modularity) and node metrics (flexibility) at different levels. The aim was to uncover dynamic network reconfiguration patterns distinct from static single-layer networks and to explore the correlations between neuroimaging markers, cognitive function, and clinical information. This research aims to provide crucial scientific evidence for the early diagnosis, intervention target screening, and auxiliary treatment of ANI patients, as well as to offer valuable insights into the neuropathophysiological mechanisms during the ANI stage.

Materials and methods

Participants

This study was approved by the Medical Ethics Committee of Beijing You'an Hospital, and all participants provided written informed consent in accordance with the Declaration of Helsinki. Given that over 90% of HIV participants in this study are right-handed males and previous studies have demonstrated a significant correlation between handedness, gender, and brain structure and function[19], our study focused on Chinese male homosexual HIV-infected individuals aged 20–50 who are right-handed. HIV infection was confirmed through Western blot or PCR methods. The exclusion criteria were as follows: (1) presence of neurological diseases that could cause cognitive impairment, such as brain tumors, infections, strokes, or epilepsy; (2) depression, anxiety, or other psychiatric disorders; (3) history of substance abuse, alcoholism, or drug addiction; (4) claustrophobia or contraindications to MRI such as pacemakers, mechanical heart valves, or defibrillators; and (5) severe visual, auditory, or reading difficulties[20]. A total of 397 HIV-infected individuals were recruited from the Sexually Transmitted Disease and AIDS Clinic at You'an Hospital, and 123 HIV-negative controls were recruited from the community.

Neuropsychological assessment

The Activities of Daily Living (ADL) scale and the Hamilton Depression Rating Scale (HAMD)[21] were used to assess whether daily living abilities were impaired and to exclude significant depressive states (HAMD score < 7). Additionally, detailed neuropsychological testing was conducted using a validated Chinese version of psychological tests normed by age, years of education, and residence[22] across six cognitive domains. The cognitive domains and corresponding neurocognitive scales are listed in Table 1. The raw scores from nine subtests were converted to normative t-scores for the six cognitive domains. According to the Frascati criteria, the diagnosis of Asymptomatic Neurocognitive Impairment (ANI) was made if: (1) performance in ≥ 2 cognitive domains was at least one standard deviation below the demographically adjusted normative mean; (2) there was no decline in daily functioning; (3) the impairment did not meet criteria for delirium or dementia; and (4) there was no evidence that the ANI was caused by other factors[3]. Among the 397 subjects, 193 were diagnosed with PWND, and 204 were diagnosed with ANI. Their cognitive performance differences are listed in Table 2.

Cognitive domains	Neurocognitive scales
Verbal and language	Animal verbal fluency test (AFT)
Attention/working memory	①Continuous performance test-identical pair (CPT-IP) ②Wechsler memory scale (WMS-III) ③Paced auditory serial addition test (PASAT)
Memory (learning and recall)	①Hopking verbal learning test (HVLT-R) ② Brief visuospatial memory test (BVMT-R)
Abstraction/executive	Wisconsin card sorting tests (WCST-64)
Speed of information processing	Trail marking test A (TMT-A)
Fine motor stills	Grooved pegboard

Table 1. Cognitive domains and corresponding neurocognitive scales.

Variable	PWND ($n=165$)	ANI ($n=173$)	HC ($n=100$)	p-value
Age(years), median(IQR)	34.0(29.0–38.0)	33.0(30.0–38.0)	32.0(28.0-36.5)	0.077[a]
Education level(years), median(IQR)	16.0(15.0–16.0)	15.0(15.0–16.0)	16.0(12.0–18)	0.110[a]
Disease course(months), median(IQR)	57.5(31.0–86.0)	52.5(29.0–74.0)	/	0.131[b]
Plasma VL(HIV RNA load)	TND	TND	/	/
$CD4^+$(cells/μl), median(IQR)	600.0(425.5–796.0)	549.0(392.0-740.0)	/	0.145[b]
$CD4^+/CD8^+$ ratio, median(IQR)	0.7(0.5–0.9)	0.6(0.4–0.9)	/	0.456[b]
Scores of cognitive performance				
Verbal and language (mean ± SD)	51.8 ± 9.3	48.2 ± 9.3	/	< 0.001[c]
Attention/working memory, median(IQR)	44.0(40.2–49.5)	37.2(32.5–42.2)	/	< 0.001[b]
Memory(learning and recall), median(IQR)	47.0(42.0–53.0)	41.0(34.0–48.0)	/	< 0.001[b]
Abstraction/executive, median(IQR)	47.0(42.5–51.5)	37.0(32.0–42.0)	/	< 0.001[b]
Speed of information processing (mean ± SD)	46.0 ± 8.2	41.3 ± 9.7	/	< 0.001[c]
Fine motor stills, median(IQR)	47.0(42.0–51.0)	44.0(39.0–51.0)	/	< 0.001[b]

Table 2. Demographic, clinical variables, and neuropsychological data. Abbreviations: A indicates the Kruskal-Wallis test, B indicates the Wilcoxon rank-sum test, and C indicates the t-test. Infection duration (months), current CD4 count, CD4/CD8 ratio, attention and working memory, memory (learning and recall), abstraction and executive function, and fine motor skills are described using medians and interquartile ranges, and compared using the Wilcoxon rank-sum test. Age and education level are described using medians and interquartile ranges, and compared using the Kruskal-Wallis test. Verbal and language skills and information processing speed are described using means and standard deviations, and compared between groups using the t-test.

Imaging acquisition

All images were acquired using a 3.0 T MRI scanner equipped with a 32-channel head coil (Siemens Trio Tim, B17 software, Erlangen, Germany). During the rs-fMRI data acquisition, participants were instructed to keep their eyes closed while remaining awake and relaxed. T1-weighted structural images were obtained using a magnetization-prepared rapid gradient echo (MP-RAGE) sequence with the following parameters: repetition time (TR) = 1900 ms, echo time (TE) = 2.52 ms, inversion time (TI) = 900 ms, acquisition matrix = 256 × 246, field of view (FOV) = 250 × 250 mm, flip angle = 9°, voxel size = 1 mm × 1 mm × 1 mm. Functional images were acquired using a gradient-echo echo-planar imaging (EPI) sequence with the following parameters: TR = 2000 ms, TE = 30 ms, acquisition matrix = 64 × 64, voxel size = 3.5 × 3.5 mm, flip angle = 90°. A total of 240 time points (35 slices) were collected over 8 min.

Imaging preprossing

Data preprocessing was conducted using the Data Processing & Analysis for Brain Imaging (DPABI, http://rfmri.org/dpabi) toolbox. To ensure signal equilibrium and participant adaptation to the environment, the first 10 time points for each subject were discarded. The remaining data underwent slice timing correction and head motion correction sequentially. Subjects with head motion greater than 3 mm or rotational motion exceeding 3° were excluded from the study. Subsequently, the resulting data were spatially normalized using T1 segmentation and transformed into the standard Montreal Neurological Institute (MNI) space. Spatial smoothing was performed using an 8 mm full-width at half maximum (FWHM) Gaussian kernel, followed by band-pass filtering ($0.01 \leq f \leq 0.1$ Hz). Finally, the potential sources of 24 head motion parameters, global signals (GS), white matter signals, and cerebrospinal fluid signals were regressed out to remove their effects. In our study, due to head motion and registration issues, imaging results from 28 PWND, 31 ANI, and 23 HC subjects were excluded.

Construction of multilayer networks

Sliding window technique was employed to divide the time series into smaller time intervals[23]. Based on previous studies, the minimum window size suitable for dynamic network analysis is determined by 1/fmin (where fmin represents the minimum frequency contained in the data)[24]. Therefore, we used a window length of 100 s (50 TRs). The sliding step was set to one time point, resulting in 181 overlapping windows. The entire brain was parcellated into 90 regions of interest (ROIs) according to the Automated Anatomical Labeling (AAL) template provided by the Montreal Neurological Institute. Time series were extracted from each ROI, defining network edges by computing Pearson correlations between average time series of node pairs. A 90 × 90 Pearson correlation matrix was constructed for each participant. Additionally, Fisher's Z transformation was applied. Pearson correlations were used to establish within-layer networks, whereas for between-layer connections, we considered connections between the same nodes across adjacent time windows to represent temporal dependencies between windows.

We employed multilayer network analysis to construct non-overlapping modularities of both temporal and spatial dimensions, enhancing dependencies between time points. This approach provided complementary information for graph-theoretical analysis to investigate the modular structure of topological networks. Each windowed segment post sliding window processing was considered a layer in our analysis. All time windows collectively formed a multilayer network, thus generating a 3D correlation matrix N×N×S (N represents the number of nodes, and S represents the total number of time windows), serving as input for an iterative Louvain community detection algorithm model. To ensure robustness against specific spatial and temporal parameters, we computed multilayer modularities using parameter sets (γ= [0.9,1,1.1], ω= [0.5,0.75,1]) for analysis[25,26]. our analysis was based on a fully connected weighted matrix to compute the global and node-level properties of the multilayer networks. Furthermore, we performed a validation analysis using a strong connection matrix with a 10% threshold to assess the stability of our results.

The model outputs two metrics: modularity index Q and node flexibility. A higher Q indicates greater network segregation, while node flexibility computes switching rates based on module transitions of nodes.

The Q calculation formula is shown in Eq. (1):

$$Q(\gamma, \omega) = \frac{1}{2\mu} \sum_{ijsr} [(A_{ijs} - \gamma_s \frac{k_{is}k_{js}}{2m_s})] \delta(M_{is}, M_{js}) + \delta(i,j)\omega_{jrs}]\delta(M_{is}, M_{jr}). \quad (1)$$

Where μ is the sum of all edge weights across nodes and layer, A_{ijs} denotes the edge strength between nodes i and j in layer s, $m_s = \frac{1}{2}\sum_{ij} A_{ij1}$ represents the total edge weight in layer s.

The topological resolution ω controls the strength of interlayer connections (larger ω implies stronger interlayer connections), while γ governs module resolution (larger γ leads to more spatial modules).

Statistical analysis

Code implementation for this experiment was conducted using Matlab. Statistical analyses were performed using IBM SPSS Statistics 29.0. A two-sample t-test was utilized to assess differences between groups for metrics including modularity index Q and node flexibility, with significance set at $p < 0.05$ and correction for multiple comparisons using the False Discovery Rate (FDR) method. Pearson correlation was employed to analyze associations between clinical information and cognitive scales, with a significance threshold set at $p < 0.05$.

Results

Demographic, clinical, and neuropsychological data

Based on the functional MRI data selection criteria, the final study included 165 PWND patients, 173 ANI patients, and 100 healthy controls (HC). Demographic, clinical characteristics, and neurocognitive test results for all patients and HCs are presented in Table 2. There were no significant differences in demographic data among the three groups. In our study, the ANI group exhibited significantly lower T scores across all six cognitive domains compared to the PWND group. These results indicate that cognitive impairment persists even in the context of viral suppression and immune recovery.

Modularity coefficient Q

The quality of communities identified by the multilayer community detection algorithm can be evaluated using the modularity Q value.We first computed the global-level properties of the multilayer networks based on a fully connected weighted matrix. The results showed that there were no statistically significant differences in modularity Q values among the three groups (Fig. 1).However, after applying a threshold to retain the top 10% of strongest connections from the fully connected matrix, the ANI group exhibited significantly lower Q values compared to the HC group across all combinations of γ and ω ($p < 0.05$). No significant differences were observed between the PWND and HC groups or between the PWND and ANI groups (Fig. 2; Table 3).

Node flexibility

We computed the node-level properties of the multilayer networks based on a fully connected weighted matrix and identified several brain regions affected by HIV infection. The spatial distribution of these altered regions is illustrated in Fig. 3. Specifically, at γ = 0.9 and ω = 0.5, the PWND group showed reduced flexibility in regions primarily within the visual (VIS) network compared to the HC group (Fig. 3A), while the ANI group exhibited reduced flexibility in regions within the default mode network (DMN), limbic system (LIM), and sensorimotor network (SMN) (Fig. 3B). At γ = 0.9 and ω = 1, the ANI group showed increased flexibility in regions mainly located in the DMN compared to the HC group (Fig. 3C). After thresholding the full connectivity matrix to retain the top 10% strongest connections, we found that the ANI group exhibited increased flexibility in the right

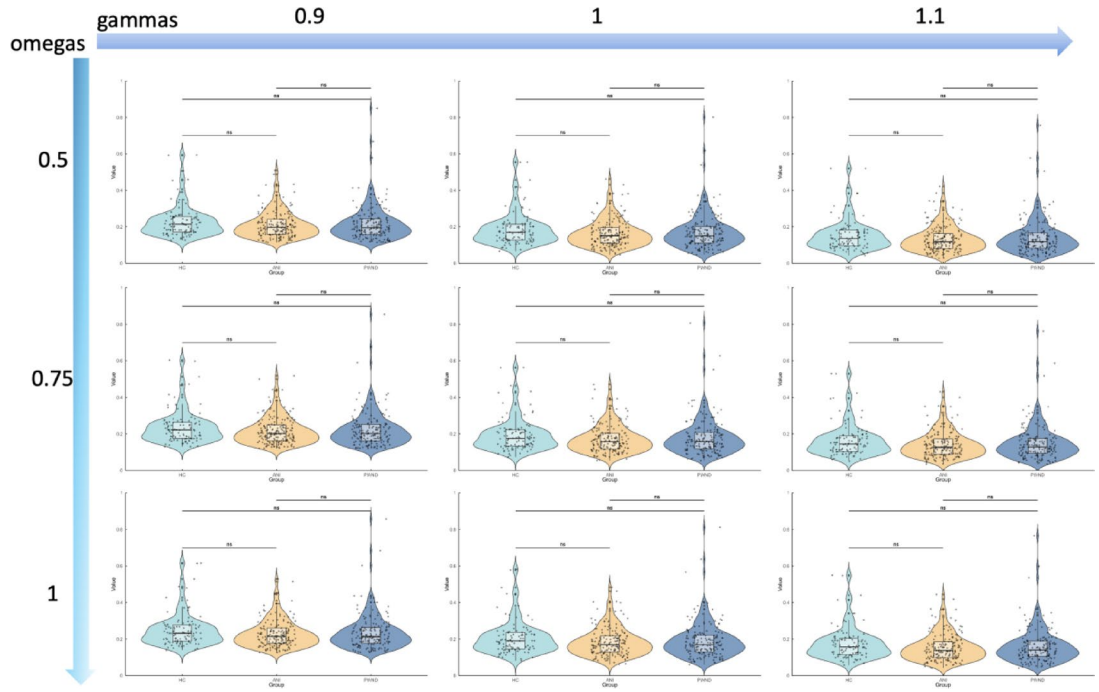

Fig. 1. Differences in modularity Q values among the three groups (full connectivity matrix). *, $p < 0.05$; ns, $p > 0.05$.

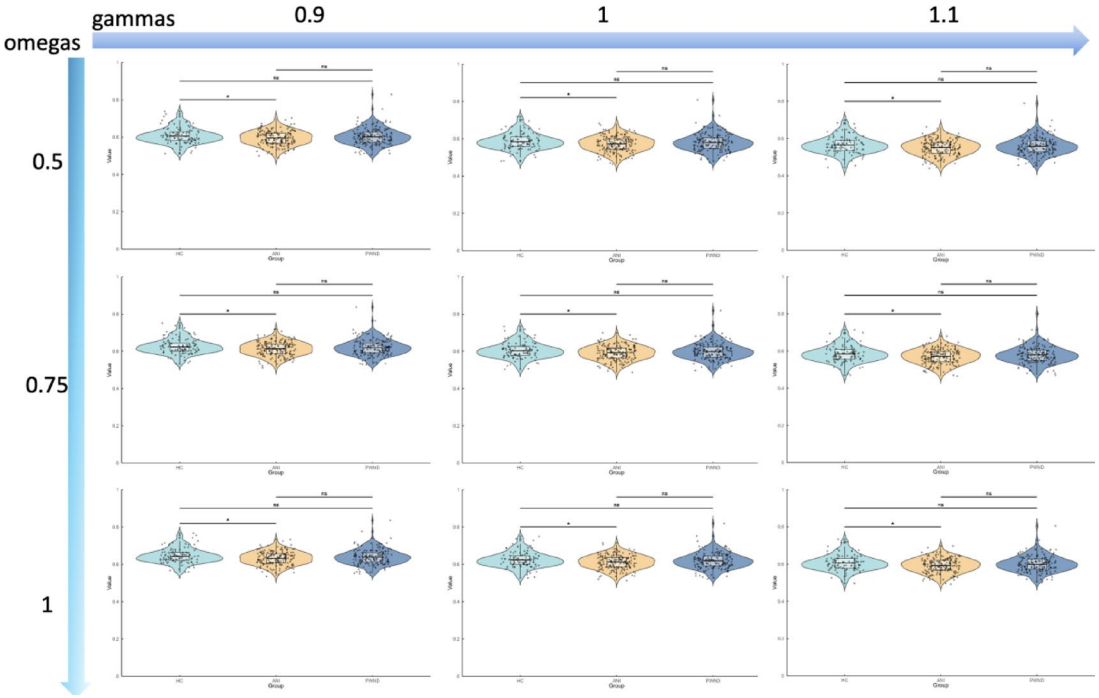

Fig. 2. Differences in modularity Q values among the three groups (top 10% strong connections). *, $p < 0.05$; ns, $p > 0.05$.

Group	Parameter	*p* value	FDR *p* value	Effect Size
ANI vs. HC	γ = 0.9, ω = 0.5	0.012	0.037	0.321
	γ = 0.9, ω = 0.75	0.011	0.034	0.324
	γ = 0.9, ω = 1	0.011	0.032	0.327
	γ = 1, ω = 0.5	0.011	0.032	0.328
	γ = 1, ω = 0.75	0.010	0.031	0.328
	γ = 1, ω = 1	0.009	0.027	0.335
	γ = 1.1, ω = 0.5	0.010	0.029	0.332
	γ = 1.1, ω = 0.75	0.010	0.030	0.330
	γ = 1.1, ω = 1	0.008	0.025	0.338

Table 3. Modularity Q value differences across parameter settings.

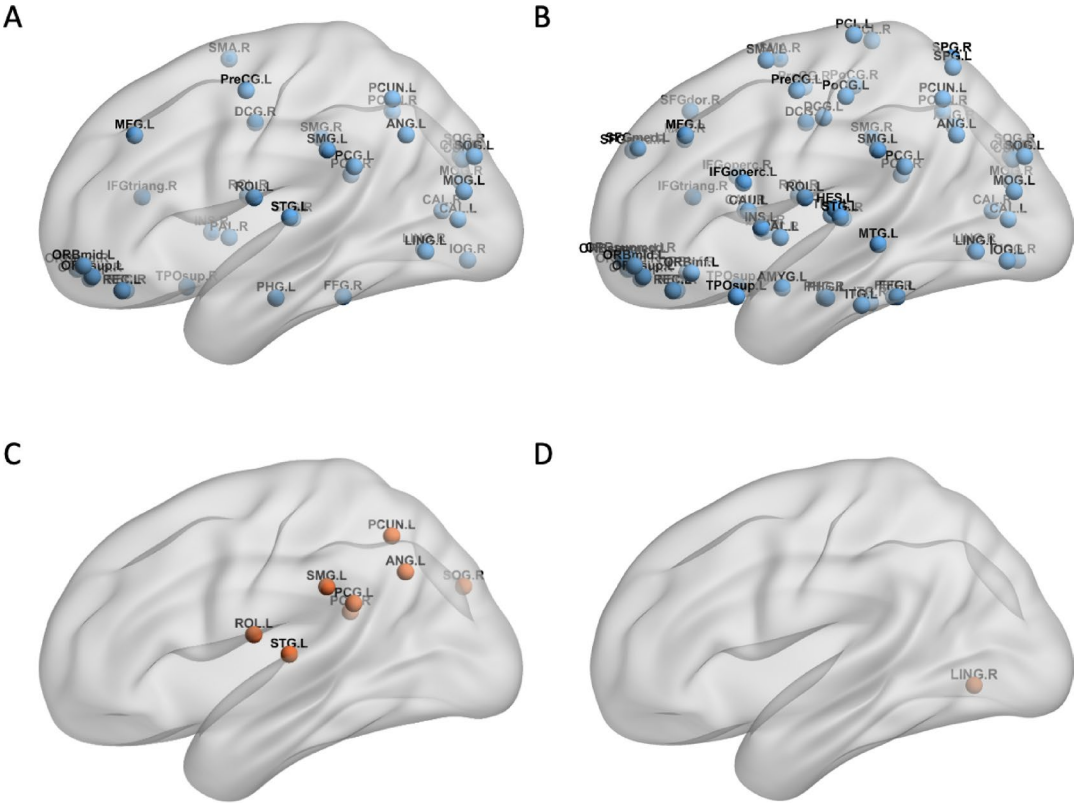

Fig. 3. Distribution of brain regions with significant differences in node flexibility among the three groups. (**A**) Brain regions with significant differences between the PWND group and the HC group (γ = 0.9, ω = 0.5). (**B**) Brain regions with significant differences between the ANI group and the HC group (γ = 0.9, ω = 0.5). (**C**) Brain regions with significant differences between the ANI group and the HC group (γ = 0.9, ω = 0.5). (**D**) Brain regions with significant differences between the ANI group and the HC group (γ = 0.9, ω = 0.5) (top 10% strong connections). Red indicates increased node flexibility; blue indicates decreased node flexibility. PWND, persons living with HIV but without neurocognitive disorders; ANI, asymptomatic neurocognitive impairment; HC, healthy control.

lingual gyrus (a region within the VIS network) compared to the HC group (Fig. 3D) (FDR corrected, $p < 0.05$). Detailed *p*-values are provided in the Supplementary Materials.

Correlation analysis results

In this study, Pearson correlation analysis was conducted to analyze the correlation between the significantly different node flexibility measures and the clinical and neurocognitive scale results of the patients. The results revealed that, at γ = 0.9 and ω = 0.5, nodal flexibility in several brain regions in the PWND group was significantly correlated with neurocognitive performance, with predominantly positive correlations (Fig. 4A). In contrast, the ANI group showed significant negative correlations between nodal flexibility and neurocognitive scores across multiple regions (Fig. 4B). At γ = 0.9 and ω = 1, in the ANI group, flexibility of the right posterior cingulate gyrus

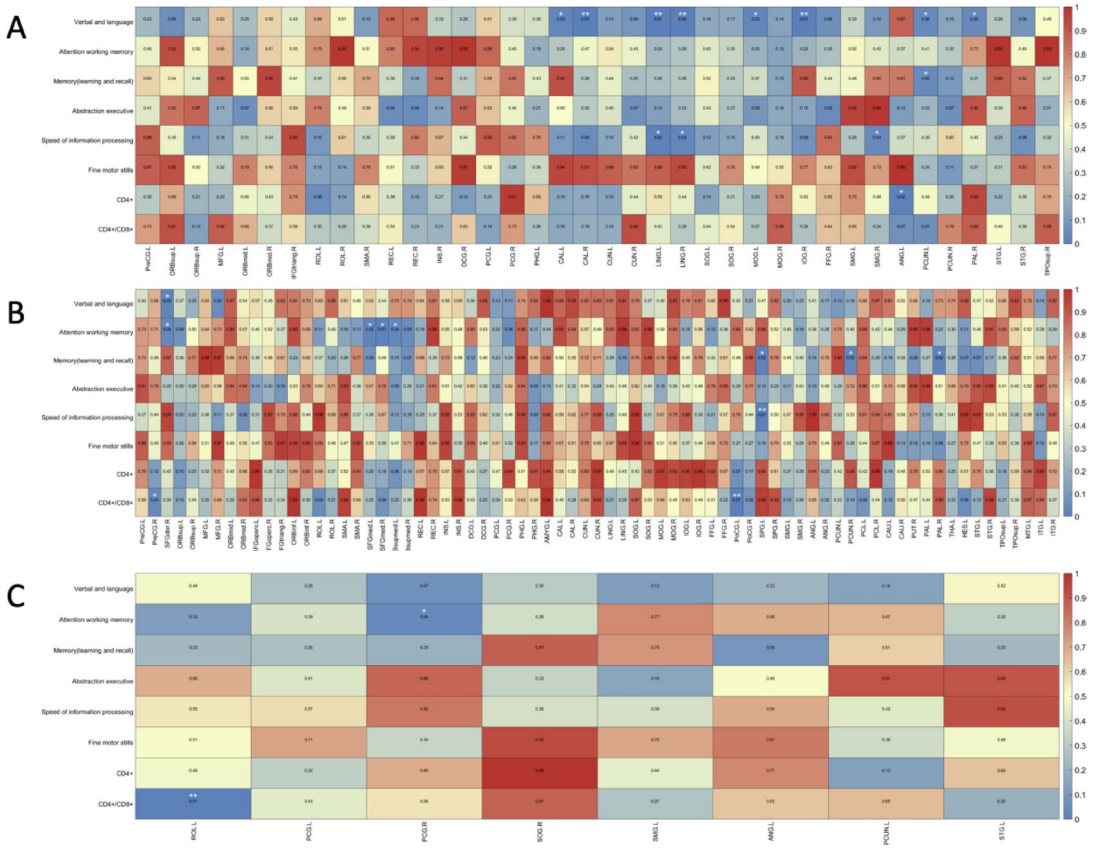

Fig. 4. Heatmap of significant correlations between nodal flexibility and clinical variables. *, $p < 0.05$; **, $p < 0.01$.

was negatively correlated with attention/working memory (r = -0.1529, $p = 0.0447$), and flexibility of the left Rolandic operculum was negatively correlated with the CD4+/CD8 + ratio (r = -0.1966, $p = 0.0095$) (Fig. 4C). However, none of these correlations survived FDR correction for multiple comparisons, and thus they should be interpreted as exploratory findings requiring further validation.

Discussion

Compared to static networks, dynamic brain networks offer enhanced sensitivity in capturing temporal fluctuations in functional connectivity, which is essential for a deeper understanding of brain activity. In this study, we leveraged a time-varying multilayer network framework—an advanced mathematical extension of traditional static networks—that enables comprehensive integration of both spatial and temporal information in neuroimaging data. This approach offers notable advantages in revealing dynamic brain alterations in patients with HIV-associated neurocognitive disorders (HAND). To systematically explore these dynamics, we introduced the following analyses: (1) Integration of temporal information: Temporal dynamics were incorporated into both the network construction and the community detection processes. This allowed us to investigate intergroup differences in brain function from the novel perspective of community dynamics, potentially offering new insights and tools for the diagnosis and treatment of HAND. (2) Evaluation of global network organization: We assessed the quality of dynamic brain network communities using the global modularity coefficient (Q). While the modularity values derived from the fully connected functional matrices showed no significant group differences, applying a 10% sparsity threshold—which retained only the strongest connections—revealed that the ANI group exhibited significantly lower modularity (Q values) than the HC group across all tested combinations of γ and ω parameters. This suggests a disruption in global community structure during the early stages of cognitive impairment. (3) Assessment of network reconfiguration: To quantify the dynamics of network reorganization, we further examined nodal flexibility, which reflects how frequently a node changes its community allegiance over time. Our results showed that: The PWND group exhibited decreased flexibility within the visual network (VIS) compared to healthy controls; The ANI group displayed widespread reductions in flexibility across multiple networks, including the default mode network (DMN), limbic system (LIM), and somatomotor network (SMN). (4) Evidence of localized reorganization: After thresholding to retain the top 10% of connections, we found increased flexibility in the right lingual gyrus (a key region in the visual network) in the ANI group. This suggests possible localized neural reorganization as a compensatory response to early HIV-related disruptions.

Network modularity reflects the extent to which a brain network can be subdivided into distinct modules, where internal connectivity is denser than would be expected by chance[27]. The quality of communities derived from multilayer community detection algorithms can be assessed using the modularity Q value. Although the theoretical range of Q spans from −1 to 1, in biological networks such as brain connectivity, Q values typically fall within 0 to 1 due to their non-random and structured organization. Lower Q values indicate poorer network segregation and modular organization, while values closer to 1 indicate stronger segregation and better-defined modular structure[15]. In our study, the lack of significant group differences in the fully connected matrix analysis may suggest that global modular organization remains relatively intact during the early or mild stages of HIV-associated cognitive impairment. In contrast, thresholding the strongest connections may more effectively capture the most stable and biologically meaningful neural signals. The observed reduction in modularity in the ANI group suggests that after HIV infection, brain regions may become relatively more isolated. Compared to healthy brain networks, the cortex in ANI patients appears to be organized into more segregated modules with diminished community integration, indicating less interregional cooperation and potentially lower cognitive efficiency[28]. In contrast, PWND patients did not show marked reductions in modularity. This could be explained by several factors. First, the brain may achieve functional integration and regulation via long-range interactions, enabling compensatory mechanisms to maintain function[29]. Previous studies have also reported evidence of such compensation in HIV patients[30]. Second, theoretical models of modularity in biological systems suggest that at short time scales, highly modular systems are more adaptive, while at longer time scales, systems with lower modularity may be favored[31]. Third, it is also possible that the PWND group includes individuals whose disease has not yet progressed, or who may never develop further HIV-related neurological symptoms. This clinical and biological heterogeneity may contribute to the absence of detectable differences in network modularity at this stage. Therefore, the long-term effects of HIV on brain network modularity warrant further longitudinal research.

Given the dynamic structure of brain connectivity, we sought to determine whether topological changes occur with HIV infection—either globally through alterations in the number or size of modules, or more locally via changes in the nodal composition of modules. Thus, we investigated nodal flexibility, which quantifies the frequency with which a node changes its community allegiance across time layers. This metric captures finer-scale fluctuations in network architecture[16] and has been identified as a biomarker of cognitive flexibility[32]. Previous studies have found that inter-individual variability in flexibility exceeds intra-individual variability, suggesting that flexibility is a reliable indicator of an individual's brain state[16]. In our results, the PWND group showed reduced flexibility primarily in the visual network, while the ANI group exhibited more extensive reductions in flexibility across the DMN, VIS, and SMN. This suggests a stronger community allegiance in these regions. Abnormalities in the visual network have been reported previously. For example, Han et al. found that the visual network is particularly vulnerable in young ANI patients[29], and Ances et al. observed significantly reduced cerebral blood flow (rCBF) in the visual cortex of HIV-infected individuals using perfusion imaging[33]. These changes may be closely related to neuronal loss in the calcarine cortex of the primary visual area[34]. The DMN, which is active at rest and involved in self-referential thinking and cognition[30], is known to be altered in numerous neurological and psychiatric conditions[35]. Previous studies have also shown that HAND can lead to disrupted functional connectivity within the DMN and between the DMN and other networks[32,35]. Alterations in the SMN have also been observed in our prior work[36]. We propose several possible explanations for these observed decreases in flexibility. First, compensatory regulation in abnormal brain regions may lead to increased activation in other areas to counterbalance reduced efficiency[1,29]. Second, prior studies suggest that regions with high flexibility may support adaptive adjustment, whereas regions with low flexibility are more likely responsible for stable functional execution[37]. Whether certain brain areas lose their adaptive capacity after prolonged HIV infection remains a topic for future investigation.

Compared to the control group, as parameters varied, particularly under conditions of higher interlayer coupling (ω), several nodes within the default mode network (DMN) in the ANI group exhibited a shift from negative to positive flexibility activation, indicating significant changes in brain state. This finding suggests the presence of dynamic reconfiguration of community structure during the resting state in ANI patients. These high-flexibility nodes continuously shift allegiance in the face of HIV invasion, leading to reduced stability of cross-layer community organization. Increased flexibility implies frequent changes in community membership, thereby reducing the stability of brain communities and reflecting the disorganization and instability of the patients' neural architecture.Such enhanced network flexibility has also been reported in other disorders. For instance, a study on the genetic risk of dynamic brain network reorganization in patients with schizophrenia found that higher flexibility reflected a lack of organizational coherence and stability in the brain network modules[17]. Similarly, Ding et al.[33] identified abnormal dynamic community structure in patients with ADHD, with significantly higher flexibility compared to controls.These results further support the critical role of the DMN in the development of HIV-associated neurocognitive disorders (HAND). DMN connectivity has also been proposed as a potential biomarker for early detection of simian immunodeficiency virus (SIV) infection and for evaluating the efficacy of antiretroviral therapy[38]. Using BOLD-fMRI, a longitudinal comparison of DMN connectivity between healthy rhesus macaques and those in the early stages of SIV infection revealed that as early as four weeks post-infection with the SIV-mac39 strain, significant alterations in functional connectivity within key DMN regions had already emerged[39].

When applying a top 10% connection threshold to extract the most representative and strongest connections from the fully connected matrix, we found that the ANI group exhibited increased flexibility in the right lingual gyrus compared to the control group. This thresholding approach helps reduce data redundancy and highlights the most functionally meaningful and stable components of brain networks, thereby minimizing noise introduced by low-correlation connections. This finding further suggests the presence of localized reorganization within neural networks associated with visual processing. The lingual gyrus, as a key node for

visual processing and top-down regulation, receives input from the primary visual cortex and is responsible for integrating information such as color, motion direction, and simple shapes[40]. Enhanced flexibility in this region implies increased communication dynamics. Previous studies have also reported functional and structural alterations of the lingual gyrus in individuals with HIV and other diseases. For example, Ma Q et al.[41] found hyperconnectivity in the right lingual gyrus of HIV patients associated with increased gray matter volume. Cognitive and gait impairments in patients with idiopathic normal pressure hydrocephalus may also be related to network damage involving the bilateral lingual gyri[42]. Additionally, patients with anxiety-depression exhibit reduced surface area in the right lingual gyrus[43], while a larger lingual gyrus volume has been linked to early responsiveness to antidepressant treatment[44].

To further elucidate the relationship between dynamic brain network characteristics and clinical cognitive performance, we performed correlation analyses between nodes with significantly altered flexibility and neurocognitive scale scores. The results revealed that under the parameter setting of $\gamma = 0.9$ and $\omega = 0.5$, multiple brain regions in the PWND group showed significant positive correlations between flexibility and cognitive scores. This suggests that, at a stage where clinical cognitive impairment has not yet manifested, brain network flexibility may serve a protective or compensatory role in maintaining normal neurocognitive functioning. In contrast, in the ANI group, decreased flexibility in several brain regions was consistently and significantly negatively correlated with neurocognitive scores under both $\gamma = 0.9$, $\omega = 0.5$ and $\omega = 1$ conditions. This widespread and consistent negative correlation implies that during the phase of neurocognitive impairment, the brain's capacity for dynamic reconfiguration is substantially compromised. The loss of network flexibility may thus be one of the key mechanisms contributing to cognitive decline. Therefore, nodal flexibility may serve not only as a dynamic indicator reflecting the state of network reorganization but also as a potential biomarker for early identification and prognosis of HIV-associated neurocognitive disorders (HAND). Moreover, the observed neuroimaging alterations did not always correspond directly to the specific cognitive functions typically associated with those brain regions but rather revealed a cross-network complexity. This could be attributed to the complexity and high-level nature of cognitive functioning, which often involves multiple parallel pathways and the coordinated regulation of several brain regions[33]. Additionally, when brain homeostasis is disrupted by disease-related cognitive impairments, brain regions exhibit considerable plasticity and may undergo reorganization to achieve functional compensation. However, it is important to note that in our correlation analyses, none of the associations between nodal flexibility and neurocognitive performance survived FDR correction, suggesting these findings should be interpreted with caution and viewed as exploratory. Lastly, the cognitive domains assessed in our study did not fully encompass all aspects of higher-order brain functions, which may have introduced some degree of bias.

Conclusion

This study is the first to investigate abnormal dynamic reconfiguration patterns of brain networks in HIV-infected individuals using a time-varying multilayer network approach, focusing on both community quality and the frequency of community reorganization. The results revealed abnormal network reconfiguration in the brains of HIV patients. Overall, significant alterations were observed in both the modularity index and the nodal flexibility of certain brain regions. These abnormalities were primarily characterized by decreased modularity and altered flexibility in specific regions, particularly within the default mode network (DMN), limbic system, sensorimotor network (SMN), and visual network. The brain states of patients appeared more unstable and prone to participating in group-wise community reorganization, and some of these abnormalities were significantly correlated with neurocognitive scale scores.These findings offer a novel perspective for understanding the working mechanisms of the brain in individuals with HIV-associated neurocognitive disorders (HAND) and provide new neuroimaging evidence for the early detection of cognitive impairment in people living with HIV (PLWH).

Limitations

This study has several limitations. Firstly, it focused exclusively on young to middle-aged male patients, which may limit the generalizability of the findings to other populations or female patients. Secondly, it was conducted at a single center with a relatively small sample size, potentially introducing selection bias. Additionally, the neuroimaging results lack pathological correlations and foundational experimental validation, necessitating confirmation in larger-scale studies. Thirdly, being cross-sectional in nature, the study is susceptible to inherent biases, and it cannot track dynamic changes in brain networks throughout disease progression. A longitudinal study would provide more robust and objective insights into these alterations.

Data availability

The data that support the findings of this study are available from the Medical Ethics Committee of Beijing Youan Hospital(No. LL-2020-0470-K) but restrictions apply to the availability of these data, which were used under license for the current study, and so are not publicly available. Data are however available from the authors upon reasonable request and with permission of the Medical Ethics Committee of Beijing Youan Hospital.

Received: 9 November 2024; Accepted: 29 May 2025
Published online: 06 June 2025

References

1. Farhadian, S., Patel, P. & Spudich, S. Neurological complications of HIV infection. *Curr. Infect. Dis. Rep.* **19**, 50 (2017).

2. Vastag, Z., Fira-Mladinescu, O. & Rosca, E. C. HIV-Associated neurocognitive disorder (HAND): Obstacles to early neuropsychological diagnosis. *Int. J. Gen. Med.* **15**, 4079–4090 (2022).
3. Antinori, A. et al. Updated research nosology for HIV-associated neurocognitive disorders. *Neurology* **69**, 1789–1799 (2007).
4. Heaton, R. K. et al. HIV-associated neurocognitive disorders persist in the era of potent antiretroviral therapy: CHARTER study. *Neurology* **75**, 2087–2096 (2010).
5. Aili, X. et al. Rich-Club analysis of structural brain network alterations in HIV positive patients with fully suppressed plasma viral loads. *Front. Neurol.* **13**, 825177 (2022).
6. Jia, C. et al. Independent component and graph theory analyses reveal normalized brain networks on Resting-State functional MRI after working memory training in people with HIV. *J. Magn. Reson. Imaging.* **57**, 1552–1564 (2023).
7. Minosse, S. et al. Functional brain network reorganization in HIV infection. *J. Neuroimaging.* **31**, 796–808 (2021).
8. De Domenico, M. Multilayer modeling and analysis of human brain networks. *Gigascience* **6**, 1–8 (2017).
9. Wang, X. et al. Deficit of Cross-Frequency integration in mild cognitive impairment and alzheimer's disease: A multilayer network approach. *J. Magn. Reson. Imaging*. **53**, 1387–1398 (2021).
10. Allen, E. A. et al. Tracking whole-brain connectivity dynamics in the resting state. *Cereb. Cortex*. **24**, 663–676 (2014).
11. Calhoun, V. D., Miller, R., Pearlson, G. & Adali, T. The chronnectome: time-varying connectivity networks as the next frontier in fMRI data discovery. *Neuron* **84**, 262–274 (2014).
12. Chen, X. et al. Extraction of dynamic functional connectivity from brain grey matter and white matter for MCI classification. *Hum. Brain Mapp.* **38**, 5019–5034 (2017).
13. Chen, X. et al. High-order resting-state functional connectivity network for MCI classification. *Hum. Brain Mapp.* **37**, 3282–3296 (2016).
14. Pedersen, M., Zalesky, A., Omidvarnia, A. & Jackson, G. D. Multilayer network switching rate predicts brain performance. *Proc. Natl. Acad. Sci. U S A*. **115**, 13376–13381 (2018).
15. Mucha, P. J., Richardson, T., Macon, K., Porter, M. A. & Onnela, J. P. Community structure in time-dependent, multiscale, and multiplex networks. *Science* **328**, 876–878 (2010).
16. Bassett, D. S. et al. Dynamic reconfiguration of human brain networks during learning. *Proc. Natl. Acad. Sci. U S A*. **108**, 7641–7646 (2011).
17. Braun, U. et al. Dynamic brain network reconfiguration as a potential schizophrenia genetic risk mechanism modulated by NMDA receptor function. *Proc. Natl. Acad. Sci. U S A*. **113**, 12568–12573 (2016).
18. He, X. et al. Disrupted dynamic network reconfiguration of the Language system in Temporal lobe epilepsy. *Brain* **141**, 1375–1389 (2018).
19. Yagi, S., Lee, A., Truter, N. & Galea, L. A. M. Sex differences in contextual pattern separation, neurogenesis, and functional connectivity within the limbic system. *Biol. Sex. Differ.* **13**, 42 (2022).
20. Chang, L. et al. Neural correlates of working memory training in HIV patients: study protocol for a randomized controlled trial. *Trials* **17**, 62 (2016).
21. Gandhi, N. S. et al. A comparison of performance-based measures of function in HIV-associated neurocognitive disorders. *J. Neurovirol.* **17**, 159–165 (2011).
22. Shi, C. et al. The MATRICS consensus cognitive battery (MCCB): Co-norming and standardization in China. *Schizophr Res.* **169**, 109–115 (2015).
23. Hindriks, R. et al. Can sliding-window correlations reveal dynamic functional connectivity in resting-state fMRI? *Neuroimage* **127**, 242–256 (2016).
24. Leonardi, N. & Van De Ville, D. On spurious and real fluctuations of dynamic functional connectivity during rest. *Neuroimage* **104**, 430–436 (2015).
25. Harlalka, V., Bapi, R. S., Vinod, P. K. & Roy, D. Atypical flexibility in dynamic functional connectivity quantifies the severity in autism spectrum disorder. *Front. Hum. Neurosci.* **13**, 6 (2019).
26. Rizkallah, J. et al. Dynamic reshaping of functional brain networks during visual object recognition. *J. Neural Eng.* **15**, 056022 (2018).
27. Newman, M. E. Modularity and community structure in networks. *Proc. Natl. Acad. Sci. U S A*. **103**, 8577–8582 (2006).
28. Iordan, A. D. et al. Aging and network properties: stability over time and links with learning during working memory training. *Front. Aging Neurosci.* **9**, 419 (2017).
29. Coelho, A. et al. Reorganization of brain structural networks in aging: A longitudinal study. *J. Neurosci. Res.* **99**, 1354–1376 (2021).
30. Melrose, R. J., Tinaz, S., Castelo, J. M., Courtney, M. G. & Stern, C. E. Compromised fronto-striatal functioning in HIV: an fMRI investigation of semantic event sequencing. *Behav. Brain Res.* **188**, 337–347 (2008).
31. Ramos-Nunez, A. I. et al. Static and dynamic measures of human brain connectivity predict complementary aspects of human cognitive performance. *Front. Hum. Neurosci.* **11**, 420 (2017).
32. Kamkwalala, A. R. et al. Brief report: higher peripheral monocyte activation markers are associated with smaller frontal and Temporal cortical volumes in women with HIV. *J. Acquir. Immune Defic. Syndr.* **84**, 54–59 (2020).
33. Damoiseaux, J. S. et al. Consistent resting-state networks across healthy subjects. *Proceedings of the National Academy of Sciences of the United States of America*. **103**(37), 13848–13853 (2006).
34. Zahr, N. M., Pohl, K. M., Pfefferbaum, A. & Sullivan, E. V. Dissociable contributions of precuneus and cerebellum to subjective and objective neuropathy in HIV. *J. Neuroimmune Pharmacol.* **14**, 436–447 (2019).
35. Hebscher, M., Ibrahim, C. & Gilboa, A. Precuneus stimulation alters the neural dynamics of autobiographical memory retrieval. *Neuroimage* **210**, 116575 (2020).
36. Jiang, X. et al. Alterations in local activity and whole-brain functional connectivity in human immunodeficiency virus-associated neurocognitive disorders: a resting-state functional magnetic resonance imaging study. *Quant. Imaging Med. Surg.* **Jan 2** (15(1)), 563–580 (2025).
37. Kim, D. et al. Overconnectivity of the right heschl's and inferior Temporal gyrus correlates with symptom severity in preschoolers with autism spectrum disorder. *Autism Res.* **14**, 2314–2329 (2021).
38. Sari, H. et al. Multimodal investigation of neuroinflammation in aviremic patients with HIV on antiretroviral therapy and HIV elite controllers. *Neurol. Neuroimmunol. Neuroinflamm Feb*. **9** (2), e1144 (2022).
39. Tang, Z. et al. The default mode network is affected in the early stage of Simian immunodeficiency virus infection: a longitudinal study. *Neural Regen Res. Jul.* **18** (7), 1542–1547 (2023).
40. Ma, Q. et al. HIV-Associated structural and functional brain alterations in homosexual males. *Front. Neurol. Jan*. **14**, 12:757374 (2022).
41. Palejwala, A. H. et al. Anatomy and white matter connections of the lingual gyrus and cuneus. *World Neurosurg. Jul.* **151**, e426–e437 (2021).
42. Suzuki, Y. et al. Reduced cerebral blood flow of lingual gyrus associated with both cognitive impairment and gait disturbance in patients with idiopathic normal pressure hydrocephalus. *J. Neurol. Sci. Jun*. **15**, 437:120266 (2022).
43. Couvy-Duchesne, B. et al. Lingual gyrus surface area is associated with anxiety-depression severity in young adults: a genetic clustering approach. *eNeuro.* **5** (1), ENEURO.0153-17.2017. (2018).
44. Jung, J. et al. Impact of lingual gyrus volume on antidepressant response and neurocognitive functions in major depressive disorder: a voxel-based morphometry study. *J. Affect. Disord Dec.* **169**, 179–187 (2014).

Acknowledgements
The authors thank all of the participants who were part of the original studies and the research staff who assisted with data collection.

Author contributions
XJ and HL conceptualized the idea. XJ, JM and CHaccessed and verified the data, performed statistical analysis. XJ wrote the manuscript and HL commented on it. All the authors participated in the critical revision of the manuscript.

Funding
This work was supported by the Beijing Hospital Authority Clinical Medicine Development Special Funding Support (ZLRK202333); National Natural Science Foundation of China (61936013, 82271963); Beijing Municipal Natural Science Foundation (7212051, L222097).

Declarations

Competing interests
The authors declare no competing interests.

Ethics approval and consent to participate
The authors are accountable for all aspects of the work in ensuring that questions related to the accuracy or integrity of any part of the work are appropriately investigated and resolved. This study was conducted in accordance with the Declaration of Helsinki (as revised in 2013) and was approved by the Medical Ethics Committee of Beijing Youan Hospital (No.LL-2020-0470-K). Written informed consent was obtained from all participants.

Additional information
Supplementary Information The online version contains supplementary material available at https://doi.org/10.1038/s41598-025-04963-9.

Correspondence and requests for materials should be addressed to H.L.

Reprints and permissions information is available at www.nature.com/reprints.

Publisher's note Springer Nature remains neutral with regard to jurisdictional claims in published maps and institutional affiliations.